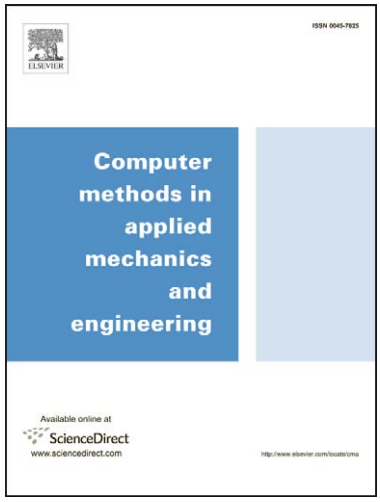
Computer Methods in Applied Mechanics and Engineering, Volume 198, Issues 30-32, 1 June 2009, Pages 2403-2411

Accepted Manuscript



Derivation of SPH Equations in a Moving Referential Coordinate System

R. Vignjevic, J. Campbell, J. Jaric, S. Powell

PII: S0045-7825(09)00098-X
DOI: 10.1016/j.cma.2009.02.027
Reference: CMA 8913

To appear in: *Comput. Methods Appl. Mech. Engrg.*

Received Date: 8 September 2008
Revised Date: 13 February 2009
Accepted Date: 19 February 2009

Please cite this article as: R. Vignjevic, J. Campbell, J. Jaric, S. Powell, Derivation of SPH Equations in a Moving Referential Coordinate System, *Comput. Methods Appl. Mech. Engrg.* (2009), doi: 10.1016/j.cma.2009.02.027

This is a PDF file of an unedited manuscript that has been accepted for publication. As a service to our customers we are providing this early version of the manuscript. The manuscript will undergo copyediting, typesetting, and review of the resulting proof before it is published in its final form. Please note that during the production process errors may be discovered which could affect the content, and all legal disclaimers that apply to the journal pertain.

ACCEPTED MANUSCRIPT

Derivation of SPH Equations in a Moving Referential Coordinate System

R. Vignjevic, J. Campbell, J. Jaric, S. Powell

Department of Applied Mechanics, School of Engineering, Cranfield University, UK

v.rade@cranfield.ac.uk

Abstract

The conventional SPH method uses kernel interpolation to derive the spatial semi-discretisation of the governing equations. These equations, derived using a straight application of the kernel interpolation method, are not used in practice. Instead the equations, commonly used in SPH codes, are heuristically modified to enforce symmetry and local conservation properties. This paper revisits the process of deriving these semi-discrete SPH equations. It is shown that by using the assumption of a moving referential coordinate system and moving control volume, instead of the fixed referential coordinate system and fixed control volume used in the conventional SPH method, a set of new semi-discrete equations can be rigorously derived. The new forms of semi-discrete equations are similar to the SPH equations used in practice. It is shown through numerical examples that the new rigorously derived equations give similar results to those obtained using the conventional SPH equations.

1 Introduction

The Smoothed Particle Hydrodynamics (SPH) method was first developed for the simulation of astrophysics problems [1], with the significant development being a method for the calculation of derivatives without a mesh. Review papers by Benz [2] and Monaghan [3] provide a thorough description of the development of the SPH method. Another important stage in the development of SPH was its extension to solid mechanics by Libersky and co-workers [4]. In the conventional SPH method the time-dependent partial differential equations, which describe conservation of mass, momentum and energy and together with a constitutive equation describe the motion of a continuum, are discretised in space using kernel interpolation.

ACCEPTED MANUSCRIPT

The approaches taken to derive the semi-discrete SPH equations can be divided into two main groups, namely variationally based and strong form based [1-6]. However, the equations derived using either approach are not in the form that is usually given in the literature. In the standard derivations, in order to ensure that the semi-discretised equations maintain conservation properties locally, additional terms are introduced into the conservation of mass equation and the conservation of linear momentum equation. The addition of these terms within the conservation equations has a heuristic nature. For instance in [6] the divergence of the velocity at particle *I* is given in terms of the values at the neighbouring *J* particles (equation 4 in reference [6]) as shown below.

$$\langle \nabla \cdot \mathbf{v}_I \rangle = \sum_J \frac{m_J}{\rho_J} (\mathbf{v}_J - \mathbf{v}_I) \cdot \nabla W_{IJ}, \tag{1.1}$$

In [6] it is noted that the term $-\mathbf{v}_I$ has been artificially added in order to ensure that the divergence vanishes for a uniform velocity distribution. Another example is the approach taken in [7] where instead of taking the direct approximation of a derivative of a function, as given by equation (1.2), the SPH form of the identity (equation 2.12 in [7]) shown below as equation (1.3) is used.

$$\left\langle \frac{\partial f_I}{\partial x} \right\rangle = \sum_J \frac{m_J}{\rho_J} f_J \frac{\partial W_{IJ}}{\partial x}, \tag{1.2}$$

$$\frac{\partial f}{\partial x} = \frac{1}{\Phi} \left(\frac{\partial (\Phi f)}{\partial x} - f \frac{\partial \Phi}{\partial x} \right). \tag{1.3}$$

This equation is a consequence of the following identity $\Phi f \equiv \Phi f$, where Φ and f are arbitrary differentiable functions of x. This identity when differentiated yields:

$$\frac{\partial (\Phi f)}{\partial x} \equiv \Phi \frac{\partial f}{\partial x} + \frac{\partial \Phi}{\partial x} f \tag{1.4}$$

Which can be rearranged to give equation (1.3). For $\Phi = 1$ equation (1.3) gives:

$$\frac{\partial f_I}{\partial x_I} = \sum_J \frac{m_J}{\rho_J} (f_J - f_I) \frac{\partial W_{IJ}}{\partial x_I}, \tag{1.5}$$

ACCEPTED MANUSCRIPT

and for $\Phi = \rho$ equation (1.3) gives

$$\frac{\partial f_I}{\partial x_I} = \frac{1}{\rho_I} \sum_J m_J \left(f_J - f_I \right) \frac{\partial W_{IJ}}{\partial x_I} . \tag{1.6}$$

From equations (1.5) and (1.6) it is obvious that the derivative approximations depend on the choice of function Φ. Substituting (1.6) into (1.5) gives:

$$\sum_J \frac{m_J}{\rho_J} \left(f_J - f_I \right) \frac{\partial W_{IJ}}{\partial x_I} = \frac{1}{\rho_I} \sum_J m_J \left(f_J - f_I \right) \frac{\partial W_{IJ}}{\partial x_I} \tag{1.7}$$

However this equality only holds if the following is true:

$$\sum_J m_J \left(\frac{1}{\rho_J} - \frac{1}{\rho_I} \right) \left(f_J - f_I \right) \frac{\partial W_{IJ}}{\partial x_I} = 0 \tag{1.8}$$

This condition states that the two approximations give the same results. For instance, in the case of arbitrary *f* and constant density ($\rho_J = \rho_I$) or constant *f* and varying ρ This approach to the derivation of the SPH equations shows the arbitrariness related to the choice of function Φ which has not yet been studied. The forms of the equations (1.5) and (1.6) derived in this way have been successfully applied to a range of problems in continuum mechanics, and so have become widely accepted. The derivation of the conventional SPH forms of the conservation equations is further discussed in Section 3.

The process of SPH discretisation of conservation equations is revisited in this paper with the intention of providing a rigorous derivation of the SPH equations. This provides a clear interpretation of the terms introduced to provide Galilean invariance. This study shows that this can be achieved through derivation of the conservation equations in a moving coordinate frame (for a moving control volume). The time-dependent partial differential equations are semi-discretised to time dependent ordinary differential equations using the following steps, that are commonly followed in SPH:

- multiplying both sides of the equation with a kernel function
- integrating all the products over the entire domain
- linearising the integrals if needed

ACCEPTED MANUSCRIPT

- Integrating each term using the technique of integration by parts. This operation moves spatial derivatives from operating on the field variables to operating on the interpolation kernel
- disregarding boundary terms
- converting all the integrals into a summation over a set of discrete particles.

2 Kernel Approximation

2.1 Overview

The SPH method is based on a kernel interpolation which in its discrete form uses distributed interpolation points, with no fixed connectivity, to approximate field variables and their spatial derivatives. In SPH, spatial derivatives are calculated by analytical differentiation of the kernel function. To illustrate this, consider a continuum represented by a set of interacting particles (Figure 1).

Each particle *I* interacts with all other particles that are within a given distance, these particles are known as neighbour particles. Parameter *h* (the smoothing length) controls this distance, all particles within *kh* of the *I* particle are neighbour particles, for the widely used B-spline kernel $k = 2$. Along with the inter-particle distance, *h* determines the spatial resolution of the calculations. The interaction between *I* and a neighbouring particle is weighted by the smoothing (or kernel) function $W(|\mathbf{x}'-\mathbf{x}|, h)$, where $\mathbf{x}'$ is the coordinate of the neighbour particle and $\mathbf{x}$ the coordinate of the *I* particle. Using this principle, the value of a continuous function can be approximated at any location within the domain based on known values at neighbouring particles *J*.

In the conventional SPH derivation of the semi-discretised form of the conservation equations, the referential coordinate system, in which the integration over the support is performed, is assumed to be fixed in space ($\mathbf{x}$ = constant, the Eulerian coordinate system). In other words, location of the support is determined by the current position of particle *I* and does not change over a given time step in the integration process. This is represented graphically in Figure 2.

2.2 The conventional SPH discretisation method

A vector function *f* can be approximated using the conventional kernel interpolation as [8]:

ACCEPTED MANUSCRIPT

$$\langle f(\mathbf{x})\rangle \approx \int_{\Omega} f(\mathbf{x}')W(|\mathbf{x}'-\mathbf{x}|,h)d\Omega \tag{2.1}$$

Where W is the kernel function, $\mathbf{x}$ is a parameter, $\mathbf{x}'$ is variable, h is the smoothing length and Ω is the kernel support centred at a point **x.**

The kernel function must satisfy the following requirements:

$W(|\mathbf{x}'-\mathbf{x}|,h)=0$ when $|\mathbf{x}'-\mathbf{x}|\geq kh$ (i.e. the Kernel should have compact support); k is a scale factor that determines size of the smoothing function support.

$W(|\mathbf{x}'-\mathbf{x}|,h)\geq 0$ in the compact support, i.e. where $|\mathbf{x}'-\mathbf{x}|\leq kh$

The integral of W over the complete support is unity:

$$\int_{\Omega} W(|\mathbf{x}'-\mathbf{x}|,h)d\Omega = 1 \tag{2.2}$$

In the limit W equals the Dirac delta function as h approaches zero.

$$\lim_{h\to 0} W(|\mathbf{x}'-\mathbf{x}|,h) = \delta(|\mathbf{x}'-\mathbf{x}|) \tag{2.3}$$

Due to the symmetric nature of the kernel function, the following expression should hold:

$$\frac{\partial W(0,h)}{\partial \mathbf{x}'} = \frac{\partial W(2h,h)}{\partial \mathbf{x}'} = 0 \tag{2.4}$$

The last requirement is very important for the treatment of boundary conditions. This property makes the derivative of approximations non-collocational, meaning that the value of the function at the location for which the derivative is being calculated, does not contribute to the approximation. Note that the kernel has to be differentiable at least once, since the kernel approximation allows spatial gradients to be determined from the values of the function and the first spatial derivative of the kernel, rather than the derivatives of the function itself. In addition, the derivative should be continuous to prevent large fluctuations in the values of the field variables of particle *I*.

The second step is to convert the kernel integrals in equation (2.1) into a volume weighted sum. This is known as particle approximation and usually stated as:

ACCEPTED MANUSCRIPT

$$
\begin{aligned}
f_I = f(\mathbf{x}_I) &\approx \langle f(\mathbf{x}_I) \rangle \\
&= \int_{\Omega} f(\mathbf{x}') W(|\mathbf{x}' - \mathbf{x}|, h) d\Omega \\
&\approx \sum_{J=1}^{N} f(\mathbf{x}_J) W_{IJ} \frac{m_J}{\rho_J}
\end{aligned}
\tag{2.5}
$$

In the previous equation, the subscript *I* and *J* denote particle number, m_J and ρ_J the mass and the density of particle *J* , *N* the number of neighbours of particle *I* (number of particles that interact with particle *I*, i.e. the support of the kernel) and $W_{IJ} = W(|\mathbf{x}_J - \mathbf{x}_I|, h)$.

Note that in the step of integral discretisation given by equation (2.5), the domain Ω of integration in the referential space (continuous integral form) is substituted by the SPH approximation $\sum_{J=1}^{N} m_J / \rho_J$ to the volume of material, which is within the referential domain of integration at that moment in time (sum form). The difference between the two domains of integration, i.e. $\Omega \neq \sum_{J=1}^{N} m_J / \rho_J$, represents one of the error sources in the process of numerical integration. This error is especially pronounced close to boundaries where the kernel support is incomplete. Due to the deformation process particles may enter and leave the neighbourhood of particle *I*, which results in a change to the approximation of the domain Ω.

A more rigorous discretisation of the spatial integral, where the neighbourhood of particle *I* is fixed, is given by equation (2.6). Here the integral over the initial referential domain is mapped onto the corresponding material domain and then discretised (converted into the sum form).

$$
\begin{aligned}
f_I = f(\mathbf{x}_I) &\approx \langle f(\mathbf{x}_I) \rangle = \int_{\Omega} f(\mathbf{x}^R) W(|\mathbf{x}^R|, \mathbf{h}) d\Omega \\
&= \int_{\Omega_0} f(\mathbf{X}^R) W(|\mathbf{X}^R|, \mathbf{h}^0) J d\Omega \\
&= \int_{\Omega_{referentieal}} f(\mathbf{x}_{ref}^R) W(|\mathbf{x}_{ref}^R|, \mathbf{h}) d\Omega \\
&\approx \sum_{J=1}^{N} f(\mathbf{x}_{ref\,J}^R) W_{IJ} (|\mathbf{x}_{ref\,J}^R|, \mathbf{h}_{IJ}^0) \frac{m_J}{\rho_J^0}
\end{aligned}
\tag{2.6}
$$

Where: $\mathbf{x}^R = \mathbf{F} \cdot \mathbf{X}^R$, $h = \mathbf{F} \cdot h^0$ and $J = \det \mathbf{F}$.

The deformation of the material domain of integration is illustrated in Figure 3. Note that at time $t = 0$ the referential and the material kernel supports are identical, and consequently there is no difference between

ACCEPTED MANUSCRIPT

the chequered (referential kernel support) and white circle (material kernel support). Whereas, at time $t = t_1$ the two domains differ due to deformation of the material kernel support. The following mappings define the link between volume of the referential and current material kernel support as $\Omega = \det \mathbf{F}\Omega_0$ and referential and current $\mathbf{h}$ as $\mathbf{h} = \mathbf{F} \cdot \mathbf{h}_0$.

This type of discretisation corresponds to, what Belytschko [9] calls the Lagrangian kernel, where the neighbourhood of an *I* particle is fixed during continuum motion and interpolation is always performed with respect to the initial configuration. It is obvious that in this case $\mathbf{h}_0$ is defined for a pair of particles and remains fixed throughout a calculation. The derivative of the kernel $W(|\mathbf{x}' - \mathbf{x}|, h)$ with respect to $\mathbf{x}$ and $\mathbf{x}'$ differs only in its sign. In the discrete form the derivative of the kernel taken with respect to $\mathbf{x}$ and $\mathbf{x}'$ are equivalent to having the kernel centred at the *I* particle (derivative with respect to **x**) or particle *J* (derivative with respect to **x**').

3 Conventional SPH Discretisation of the Equations of Conservation

In SPH, a time-dependent partial differential equation is converted into a time dependent ordinary differential equation by following the steps given in the introduction. In this section the conventional discretisation of the SPH equations is presented, this will allow comparison with the derivation of the equations in a moving referential frame presented in the next section.

3.1 Conservation of Mass

The conservation of mass equation is to be considered first. Starting from the partial differential equation

$$\frac{D\rho}{Dt} = -\rho \nabla \cdot \mathbf{v} \tag{3.1}$$

Where the material time derivative is taken in a fixed reference frame, Figure 2.

The first steps are to multiply both sides of the equation by the smoothing function, then integrate over the domain of particle *I*. After linearization, following Libersky [10], of the resulting integral one obtains:

ACCEPTED MANUSCRIPT

$$\int_{\Omega} W(|\mathbf{x}'-\mathbf{x}|,h)\left.\frac{D\rho}{Dt}\right|_x d\Omega \approx -\rho_I \int_{\Omega} W(|\mathbf{x}'-\mathbf{x}|,h)\nabla\cdot\mathbf{v}d\Omega \tag{3.2}$$

Integrating by parts and dropping boundary terms yields:

$$\left\langle \frac{D\rho_I}{Dt} \right\rangle = \int_{\Omega} W(|\mathbf{x}'-\mathbf{x}|,h)\left.\frac{D\rho}{Dt}\right|_x d\Omega \approx \rho_I \int_{\Omega} \mathbf{v}\cdot\nabla W(|\mathbf{x}'-\mathbf{x}|,h)d\Omega \tag{3.3}$$

Converting the integral into a discrete sum over the set of neighbour particles then gives:

$$\left\langle \frac{D\rho_I}{Dt} \right\rangle = \rho_I \sum_J \frac{m_J}{\rho_J}\mathbf{v}_J\cdot\nabla W_{IJ} \tag{3.4}$$

This however, is not the usual form of the discretised SPH equation often found in literature [1, 2]. In order to maintain Galilean invariance (in the case of the conservation of mass equation) and to ensure the satisfaction of Newton's third law (in the case of the momentum equation), an additional term is introduced into Equation (3.2). This term has the following form:

$$\rho_I \int_{\Omega} \mathbf{v}_I\cdot\nabla W(|\mathbf{x}'-\mathbf{x}|,h)d\Omega \approx \rho_I \mathbf{v}_I\cdot\sum_J \frac{m_J}{\rho_J}\nabla W_{IJ} \tag{3.5}$$

Note that this term in its continuous form is equal to zero due to the symmetric nature of the smoothing function *W*. Subtracting this expression above from the right hand side of equation (3.4) yields

$$\langle \dot{\rho}_I \rangle = \rho_I \sum_J (\mathbf{v}_J - \mathbf{v}_I)\nabla W \frac{m_J}{\rho_J} \tag{3.6}$$

3.2 Conservation of Momentum

The momentum equation in the spatial form, neglecting surface distributed forces and body forces is:

$$\frac{\partial(\rho\mathbf{v})}{\partial t} + \nabla(\rho\mathbf{v}\otimes\mathbf{v}) = \rho\frac{D\mathbf{v}}{Dt} = \nabla\cdot\sigma \tag{3.7}$$

Multiplying both sides by the smoothing function and integrating over the domain yields:

$$\int_{\Omega} \frac{D\mathbf{v}}{Dt} W(|\mathbf{x}'-\mathbf{x}|,h)d\Omega = \int_{\Omega} \frac{\nabla\cdot\sigma}{\rho} W(|\mathbf{x}'-\mathbf{x}|,h)d\Omega \tag{3.8}$$

Integration by parts and dropping boundary terms yields

ACCEPTED MANUSCRIPT

$$\left\langle \frac{D\mathbf{v}}{Dt} \right\rangle \approx -\int_{\Omega} \frac{1}{\rho} \sigma \cdot \nabla W(|\mathbf{x}' - \mathbf{x}|, h) d\Omega \tag{3.9}$$

The integral is then approximated by a particle sum:

$$\left\langle \frac{D\mathbf{v}_I}{Dt} \right\rangle = -\sum_J \frac{m_J}{\rho_J} \frac{\sigma_J}{\rho_J} \cdot \nabla W_{IJ} \tag{3.10}$$

To ensure Newton's third law is met locally, the equation is modified to give:

$$\left\langle \frac{D\mathbf{v}_I}{Dt} \right\rangle = -\sum_J m_J \left(\frac{\sigma_I}{\rho_I^2} + \frac{\sigma_J}{\rho_J^2} \right) \cdot \nabla W_{IJ} \tag{3.11}$$

The full meaning of these heuristic changes to the discretised conservation equations has not previously been explained. The derivation presented in the next section offers an explanation of the form of equations (3.6) and (3.11).

4 SPH Discretisation in a Moving Referential Frame

In order to express the conservation equations in a referential domain, the approach similar to the general theory developed by Hughes et al [11] for the Lagrangian, Eulerian and mixed descriptions of continuum motion was used.

The following assumptions provide the basis for the SPH semi-discretisation of the conservation equations that follows:

- Kernel interpolation (integration) is performed in a set of moving referential coordinate systems, each attached to a particle I ($1 \le I \le$ number of particles).
- The translational velocity of each referential coordinate system is identical to the velocity of the I particle to which it is attached.
- The smoothing length h of the interpolation function (centred at particle I) stays constant throughout the calculation.

It is important to note that, the continuum occupying a kernel support moves relative to the referential coordinate system everywhere, apart from the location coinciding with the particle I. Consequently, when the

ACCEPTED MANUSCRIPT

kernel interpolation integral is discretised, the mass assigned to particle *I* cannot leave kernel support for the particle.

Another possible interpretation of the kernel support is that it represents a variable-mass system (an open system or a system of changing composition). To be precise kernel support is a *control volume* enclosed by a *control surface*. Although the shape of the control volume is assumed to be fixed, the matter within the control volume may change with time.

Neighbouring *J* particles ($1 \le J \le$ number of neighbours) move relative to the referential coordinate system with a velocity $\mathbf{v}_R = \mathbf{v}_J - \mathbf{v}_I$, where $\mathbf{v}_J$ is the velocity of particle *J* and $\mathbf{v}_I$ is the velocity of particle *I*. Note, the mass assigned to *J* particles can leave the kernel support of *I* particle.

To start, a moving referential (Cartesian) frame is attached to the particle *I*. In doing so the distance $|\mathbf{x}' - \mathbf{x}|$ that the kernel function *W* depends on, becomes a function of two variables, $\mathbf{x}$ and $\mathbf{x}'$.

The smoothing length *h* of the interpolation function (centred at particle *I*) defines the kernel support or control volume (*CV*) over which the smoothing is performed. In general, the continuum occupying the *CV* moves relative to the *CV* everywhere apart from the location defined by $\mathbf{x}$ with relative velocity, $\mathbf{v}_R = \frac{d\mathbf{x}_R}{dt} = \frac{d(\mathbf{x}' - \mathbf{x})}{dt}$. In the case of the discrete form, neighbouring particles move relative to the referential frame and the control volume with a velocity, $\mathbf{v}_R = \frac{d\mathbf{x}_R}{dt} = \mathbf{v}_J - \mathbf{v}_I$, where $\mathbf{v}_J$ is the velocity of a material point within the *CV* and $\mathbf{v}_I$ is the velocity of the referential coordinate system attached to particle *I*. In other words, the velocity of the referential frame and the *CV* is identical to the velocity of particle *I*. This is represented schematically in Figure 4.

4.1 Properties of the referential derivative

There are two properties of the referential derivative that need to be shown before deriving the revised conservation of mass and momentum equations. However, first it is useful to recollect the expressions for the material derivatives in the spatial and the referential systems, given by equations (4.1) and (4.2) respectively.

ACCEPTED MANUSCRIPT

$$\frac{Df}{Dt} = \frac{\partial f}{\partial t} + \mathbf{v} \cdot \nabla f \tag{4.1}$$

$$\frac{\tilde{D}f}{Dt} = \frac{\partial f}{\partial t} + \mathbf{v}_{CV} \cdot \nabla f \tag{4.2}$$

Where $\mathbf{v}$ is the velocity of a material point within the control volume and $\mathbf{v}_{CV}$ is the velocity of the control volume (identical to the velocity of the material point at the origin of the moving coordinate system).

The relation between these material derivatives, for any point **x**' within the *CV*, follows from the above equations:

$$\frac{Df}{Dt} = \underbrace{\frac{\tilde{D}f}{Dt}}_{referential} + \mathbf{v}_R \cdot \nabla f \tag{4.3}$$

In the above equation $\mathbf{v}_R = \frac{d\mathbf{x}_R}{dt} = \frac{d(\mathbf{x}' - \mathbf{x})}{dt} = \mathbf{v} - \mathbf{v}_{CV}$ is the relative velocity or the velocity of the material point with respect to the referential coordinate system.

First property

The first property of the referential derivative as described above is:

$$\int_\Omega \frac{\tilde{D}}{Dt} f dv = \frac{\tilde{D}}{Dt} \int_\Omega f dv \tag{4.4}$$

Proof: Starting from the definition of material derivative

$$\frac{D}{Dt} \int_\Omega f dv = \int_\Omega \left(\frac{Df}{Dt} + f \nabla \cdot \mathbf{v} \right) dv \tag{4.5}$$

Next, writing (4.3) in integral form one obtains

$$\int_\Omega \frac{\tilde{D}}{Dt} f dv = \int_\Omega \frac{D}{Dt} f dv - \int_\Omega \mathbf{v}_R \cdot \nabla f dv \tag{4.6}$$

The second term on the right hand side in equation (4.6) can be expanded as,

$$\int_\Omega \mathbf{v}_R \cdot \nabla f dv = \int_\Omega \nabla \cdot (f \mathbf{v}_R) dv - \int_\Omega f \nabla \cdot \mathbf{v}_R dv \tag{4.7}$$

ACCEPTED MANUSCRIPT

$$= \int_{\partial\Omega} f\, \mathbf{v}_R \cdot \mathbf{n} da - \int_{\Omega} f \nabla \cdot \left(\mathbf{v} - \mathbf{v}_{CV} \right) dv$$

$$= \int_{\partial\Omega} f\, \mathbf{v}_R \cdot \mathbf{n} da - \int_{\Omega} f \nabla \cdot \mathbf{v} dv$$

Because, the referential frame is moving with velocity $\mathbf{v}_{CV}$ the simplification in the last row of equation (4.7) can be performed as a consequence of the fact that divergence of a constant velocity field is zero, i.e. $\nabla \cdot \mathbf{v}_{CV} = 0$. Substituting the last row of equation (4.7) into equation (4.6) yields:

$$\int_{\Omega} \frac{\tilde{D}}{Dt} f dv = \int_{\Omega} \left(\frac{Df}{Dt} + f \nabla \cdot \mathbf{v} \right) dv - \int_{\partial\Omega} f\, \mathbf{v}_R \cdot \mathbf{n} da$$

To complete the proof, the expression for material derivative given in equation (4.5) is then substituted into the above equation:

$$\begin{aligned} &= \frac{D}{Dt} \int_{\Omega} f dv - \int_{\partial\Omega} f\, \mathbf{v}_R \cdot \mathbf{n} da \\ &= \frac{\tilde{D}}{Dt} \int_{\Omega} f dv \end{aligned} \tag{4.8}$$

Second property

If one assumes that in the referential coordinate system the domain of integration (control volume) $\tilde{\Omega}$, is attached to a material point x_i, and that it coincides with the material domain Ω ($\tilde{\Omega} \equiv \Omega$) at that point in time, then the following holds:

$$\frac{D}{Dt} \int_{\Omega} f dv = \int_{\tilde{\Omega}} \frac{\tilde{D}}{Dt} f dv \tag{4.9}$$

Proof: In order to prove assertion (4.9) one can start from material derivative:

$$\frac{D}{Dt} \int_{\Omega} f dv = \int_{\Omega} \left(\frac{Df}{Dt} + f \nabla \cdot \mathbf{v} \right) dv \tag{4.10}$$

Next, using equation (4.6) the above equation can be rewritten as:

$$\int_{W} \frac{\tilde{D}}{Dt} f dv = \int_{W} \frac{D}{Dt} f dv - \int_{\Omega} \mathbf{v}_R \cdot \nabla f dv \tag{4.11}$$

Having in mind that:

ACCEPTED MANUSCRIPT

$$\int_{\Omega} \mathbf{v}_R \cdot \nabla f dv = \int_{\Omega} \nabla \cdot \left(f \, \mathbf{v}_R \right) dv - \int_{\Omega} f \, \nabla \cdot \mathbf{v}_R dv =$$
$$= \int_{\Omega} f \, \mathbf{v}_R \cdot \mathbf{n} da - \int_{\Omega} f \, \nabla \cdot \left(\mathbf{v} - \mathbf{v}_{CV} \right) dv = \int_{\partial\Omega} f \, \mathbf{v}_R \cdot \mathbf{n} da - \int_{\Omega} f \, \nabla \cdot \mathbf{v} dv \tag{4.12}$$

Using the fact that $\nabla \cdot \mathbf{v}_{CV} = 0$, one can proceed to write

$$\int_{\Omega} \frac{\tilde{D}}{Dt} f dv = \int_{\Omega} \left(\frac{D}{Dt} f + f \, \nabla \cdot \mathbf{v} \right) dv - \int_{\partial\Omega} f \, \mathbf{v}_R \cdot \mathbf{n} da =$$
$$\frac{D}{Dt} \int_{\Omega} f dv - \int_{\partial\Omega} f \, \mathbf{v}_R \cdot \mathbf{n} da = \frac{\tilde{D}}{Dt} \int_{\Omega} f dv \tag{4.13}$$

This completes the proof.

4.2 Conservation of Mass

To discretise the continuity equation in space two approaches were considered. In the first approach the equation is discretised starting from the local form of the continuity in the spatial coordinate system. In the second the integral form of the continuity equation for the moving *CV* is considered.

Using equation (4.3), the continuity equation (3.1) can be rewritten for the referential coordinate system as:

$$\frac{\tilde{D}\rho}{Dt} + \rho \nabla \cdot \mathbf{v} + \mathbf{v}_R \cdot \nabla \rho = 0 \tag{4.14}$$

Depending on the process followed, different discrete forms of the continuity equation can be derived. To demonstrate this two different discrete forms of equation 4.14 are derived below.

Form 1

Writing $\mathbf{v}_R = \mathbf{v} - \mathbf{v}_{CV}$ (where $\mathbf{v}_{CV}$ is the velocity of the referential system and the control volume attached to it) and substitute into (4.13) gives:

$$\frac{\tilde{D}\rho}{Dt} + \rho \nabla \cdot \mathbf{v} + (\mathbf{v} - \mathbf{v}_{CV}) \cdot \nabla \rho$$
$$= \frac{\tilde{D}\rho}{Dt} + \rho \nabla \cdot \mathbf{v} + \mathbf{v} \cdot \nabla \rho - \mathbf{v}_{CV} \cdot \nabla \rho \tag{4.15}$$
$$= \frac{\tilde{D}\rho}{Dt} + \nabla \cdot (\rho \mathbf{v}) - \mathbf{v}_{CV} \cdot \nabla \rho$$

ACCEPTED MANUSCRIPT

Multiplication of the above equation by the kernel function and integration over the domain yields:

$$\int_{\Omega} \frac{\tilde{D}\rho}{Dt} W(|\mathbf{x}'-\mathbf{x}|,h)d\Omega + \int_{\Omega} \nabla\cdot(\rho\mathbf{v}) W(|\mathbf{x}'-\mathbf{x}|,h)d\Omega - \\ -\int_{\partial\Omega} \mathbf{v}_{CV}\cdot\nabla\rho W(|\mathbf{x}'-\mathbf{x}|,h)d\Omega = 0 \tag{4.16}$$

After integration by parts and neglecting the boundary terms one finds:

$$\langle\dot{\rho}\rangle - \int_{\Omega} \rho\mathbf{v}\cdot\nabla W(|\mathbf{x}'-\mathbf{x}|,h)d\Omega + \mathbf{v}_I \int_{\Omega} \rho\nabla W(|\mathbf{x}'-\mathbf{x}|,h)d\Omega = 0 \tag{4.17}$$

Where $\langle\dot{\rho}\rangle = \int_{\Omega} \frac{\tilde{D}\rho}{Dt} W(|\mathbf{x}'-\mathbf{x}|,h)d\Omega$. When discretised the above equation can be written as:

$$\langle\dot{\rho}\rangle - \sum_J \rho_J \frac{m_J}{\rho_J}\mathbf{v}_J\cdot\nabla(W_{IJ}) + \mathbf{v}_I \sum_J \rho_J \frac{m_J}{\rho_J}\nabla(W_{IJ}) = 0 \tag{4.18}$$

$$\langle\dot{\rho}\rangle = -\sum_J m_J(\mathbf{v}_J - \mathbf{v}_I)\cdot\nabla(W_{IJ})$$

Alternatively starting from the global conservation of mass in the moving reference frame (3.1) one can write

$$\frac{D}{Dt}\int_{\tilde{\Omega}} \rho dv = \int_{\delta\tilde{\Omega}} \rho\mathbf{v}_R\cdot\mathbf{n} = \int_{\tilde{\Omega}} \nabla(\rho\mathbf{v}_R)dv \\ \int_{\tilde{\Omega}} \frac{\tilde{D}}{Dt}\rho dv - \int_{\tilde{\Omega}} \nabla(\rho\mathbf{v}_R)dv = 0 \tag{4.19}$$

$$\frac{\tilde{D}}{Dt}\rho = \nabla(\rho\mathbf{v}_R)$$

One can then proceed as normal, multiplication by a kernel, integration by parts and discretisation which yields:

$$\langle\dot{\rho}\rangle = -\sum_J m_J(\mathbf{v}_J - \mathbf{v}_I)\cdot\nabla(W_{IJ}) \tag{4.20}$$

Form 2

Multiplying equation (4.10) by the kernel function and integrating over the domain yields

ACCEPTED MANUSCRIPT

$$\int_{\Omega}\frac{\tilde{D}\rho}{Dt}W(|\mathbf{x}'-\mathbf{x}|,h)d\Omega+\int_{\Omega}\rho\nabla\mathbf{v}W(|\mathbf{x}'-\mathbf{x}|,h)d\Omega+\int_{\Omega}\mathbf{v}_R\nabla\rho W(|\mathbf{x}'-\mathbf{x}|,h)d\Omega=0 \tag{4.21}$$

After integration by parts and neglecting the boundary terms one finds

$$\begin{aligned}\langle\dot{\rho}\rangle=&\int_{\Omega}\mathbf{v}\rho\nabla W(|\mathbf{x}'-\mathbf{x}|,h)d\Omega+\int_{\Omega}\mathbf{v}\cdot\nabla\rho W(|\mathbf{x}'-\mathbf{x}|,h)d\Omega\\&+\int_{\Omega}\rho\nabla\cdot\mathbf{v}_R W(|\mathbf{x}'-\mathbf{x}|,h)d\Omega+\int_{\Omega}\rho\mathbf{v}_R\cdot W(|\mathbf{x}'-\mathbf{x}|,h)d\Omega\end{aligned} \tag{4.22}$$

Grouping of terms in (4.22) gives

$$\begin{aligned}\langle\dot{\rho}\rangle=&\int_{\Omega}(2\mathbf{v}-\mathbf{v}_{CV})\rho\nabla W(|\mathbf{x}'-\mathbf{x}|,h)d\Omega+\int_{\Omega}\mathbf{v}\nabla\rho W(|\mathbf{x}'-\mathbf{x}|,h)d\Omega\\&+\int_{\Omega}\rho\nabla\mathbf{v}_R W(|\mathbf{x}'-\mathbf{x}|,h)d\Omega\end{aligned} \tag{4.23}$$

The second and third integrals in the above expression can be linearised using Taylor expansion:

$$\begin{aligned}\langle\dot{\rho}\rangle\approx&\int_{\Omega}(2\mathbf{v}-\mathbf{v}_{CV})\rho\nabla W(|\mathbf{x}'-\mathbf{x}|,h)d\Omega+\mathbf{v}\int_{\Omega}\nabla\rho W(|\mathbf{x}'-\mathbf{x}|,h)d\Omega\\&+\rho\int_{\Omega}\nabla\mathbf{v}_R W(|\mathbf{x}'-\mathbf{x}|,h)d\Omega\end{aligned} \tag{4.24}$$

Then partial integration of the linearised terms yield the final continuous form of the continuity equation:

$$\begin{aligned}\langle\dot{\rho}\rangle=&\int_{\Omega}(2\mathbf{v}-\mathbf{v}_{CV})\rho\nabla W(|\mathbf{x}'-\mathbf{x}|,h)d\Omega-\mathbf{v}\int_{\Omega}\rho\nabla W(|\mathbf{x}'-\mathbf{x}|,h)d\Omega\\&-\rho\int_{\Omega}(\mathbf{v}-\mathbf{v}_{CV})\nabla W(|\mathbf{x}'-\mathbf{x}|,h)d\Omega\end{aligned} \tag{4.25}$$

When discretised the above equation can be written as:

$$\begin{aligned}\langle\dot{\rho}\rangle=&\sum_J(2\mathbf{v}_J-\mathbf{v}_I)\rho_J\nabla W_{IJ}\frac{m_J}{\rho_J}-\mathbf{v}_I\sum_J\rho_J\nabla W_{IJ}\frac{m_J}{\rho_J}\\&-\rho_I\sum_J(\mathbf{v}_J-\mathbf{v}_I)\nabla W_{IJ}\frac{m_J}{\rho_J}\end{aligned} \tag{4.26}$$

This then simplifies to

$$\langle\dot{\rho}\rangle=\sum_J\frac{2\rho_J-\rho_I}{\rho_J}m_J(\mathbf{v}_J-\mathbf{v}_I)\nabla W_{IJ} \tag{4.27}$$

ACCEPTED MANUSCRIPT

4.3 Conservation of Momentum

In the consideration of the momentum equation presented below, a similar approach as with the conservation of mass equation was taken. Using equation (4.3) one can rewrite the momentum equation (3.7) as

$$\frac{\tilde{D}\mathbf{v}}{Dt} + \mathbf{v}_R \cdot \nabla \mathbf{v} = \frac{1}{\rho} \nabla \cdot \sigma \tag{4.28}$$

Multiplication of the above equation by the kernel function and integration over the domain yields:

$$\int_\Omega \frac{\tilde{D}\mathbf{v}}{Dt} W(|\mathbf{x}' - \mathbf{x}|, h) d\Omega + \int_\Omega \nabla \cdot \mathbf{v}\mathbf{v}_R W(|\mathbf{x}' - \mathbf{x}|, h) d\Omega = \frac{1}{\rho} \int_\Omega \nabla \cdot \sigma W(|\mathbf{x}' - \mathbf{x}|, h) d\Omega \tag{4.29}$$

Using the divergence theorem, and after dropping the boundary terms, this transforms into the form convenient for discretisation (note, the velocity in the second term is linearised):

$$\begin{aligned} &\langle \dot{\mathbf{v}} \rangle + \mathbf{v} \int_\Omega \nabla \mathbf{v}_R W(|\mathbf{x}' - \mathbf{x}|, h) d\Omega - \int_\Omega \mathbf{v}(\mathbf{v}_R \cdot \nabla W(|\mathbf{x}' - \mathbf{x}|, h)) d\Omega = \\ &= \frac{1}{\rho} \int_\Omega \nabla \cdot \sigma W(|\mathbf{x}' - \mathbf{x}|, h) d\Omega \end{aligned} \tag{4.30}$$

When discretised the above equation can be written as:

$$\begin{aligned} &\langle \dot{\mathbf{v}}_I \rangle + \sum_J \mathbf{v}_I \frac{m_J}{\rho_J} (\mathbf{v}_R \cdot \nabla W_{IJ}) - \sum_J \mathbf{v}_J \frac{m_J}{\rho_J} (\mathbf{v}_R \cdot \nabla W_{IJ}) \\ &= -\frac{1}{\rho_I} \sum_J (\sigma_I + \sigma_J) \frac{m_J}{\rho_J} \nabla W_{IJ} \end{aligned} \tag{4.31}$$

This then simplifies to:

$$\begin{aligned} \langle \dot{\mathbf{v}}_I \rangle = &\sum_J \frac{m_J}{\rho_J} (\mathbf{v}_J - \mathbf{v}_I)(\mathbf{v}_R \cdot \nabla W_{IJ}) - \\ &- \frac{1}{\rho_I} \sum_J \frac{m_J}{\rho_J} (\sigma_I + \sigma_J) \nabla W_{IJ} \end{aligned} \tag{4.32}$$

The discrete form of the conservation of momentum equation (4.32) differs from the equation (3.11) by the first term on the right hand side. Note, that the magnitude of this term remains small while the relative velocity between the *I* particle and its neighbouring *J* particles is low.

ACCEPTED MANUSCRIPT

5 Numerical Examples

To investigate the new forms of the SPH equations, the continuity equation (4.27) and the momentum equation (4.32) were implemented into our in-house SPH code. Two numerical examples, a 1D shock tube example and a 2D elastic-plastic impact problem are given below to illustrate the performance of these new forms. The Sod shock tube problem is a widely used test case in compressible gas dynamics [13] and a symmetric elastic-plastic block impact has been previously published [14-16].

The conventional SPH form of semi-discretised equations and the newly developed form were discretised in time using the same central difference scheme. The same central-difference scheme is widely used in explicit finite element codes [17]. The time step size is variable and controlled by the stability requirements of the explicit scheme. The Courant number of the shock tube was kept at 0.6 for the shock tube problem and 0.8 for the symmetric block impact. A smaller step size was used for the Sod problem due to the presence of a strong shock. A standard von Neumann-Richtmyer pressure form of the artificial viscosity was used with linear coefficient 0.06 and quadratic coefficient 1.5.

5.1 1D Shock tube test

To compare the new framework to conventional SPH in 1D the Sod shock tube problem was considered. The problem definition and initial conditions are shown in Figure 5. The model comprises 100 particles in total, 50 on each side of the initial interface discontinuity. The gas is modelled using the perfect gas equation of state with $\gamma = 1.4$. This problem generates a shock that travels to the right, and an expansion fan to the left. As can be seen in Figures 6 and 7 the results from the two formulations are very similar.

No special treatment of the contact discontinuity has been used, to keep the comparison of the behaviour of the two forms of discrete equations simple. This results in oscillation at the contact discontinuity that forms during the very first time steps of the solution. As this is a collocational scheme these zero-energy mode oscillations persist in the solution [15].

5.2 2D Block impact problem

To compare the behaviour of the two frameworks in higher dimensions, a normal symmetrical impact of two metallic blocks was simulated in 2D. Each block was 1.0cm x 0.4 cm, see Figure 9, and modelled using 50 x 20 particles. A bi-linear elastic-plastic material model [17] was used for each block, with material properties

ACCEPTED MANUSCRIPT

given in table 1. The two sets of results, shown in Figure 9 to Figure 11, are very similar. The level of the actual differences are larger than seen in the 1D shock tube problem, but remain small with the maximum difference in total kinetic energy below 1.5%.

The two tests show that the new form of the conservation equations gives simulation results that compare well with the conventional SPH method for problems where the relative velocity between neighbour particles is small. Further work is required to test and demonstrate the new framework on problems where the relative velocity is large.

6 Conclusions

A framework for the SPH semi-discretisation of the conservation equations, where kernel interpolation is performed in the moving reference frame attached to particle *I*, was developed.

The new framework allows for a rigorous SPH semi-discretisation of the conservation equations without the need for any heuristic changes to the equations. The analysis presented offers a possible explanation for the form of the semi-discrete SPH equations in common use, in that they represent the conservation laws written in a moving reference frame. The continuous form of the conservation equations can be discretised in a number of ways. The new form of the conservation equations considered here compares well with the conventional SPH forms of the equations for the numerical examples considered, with differences in the results for the 2D being generally less than 1%.

The presented approach provides a framework for the future derivation of semi discretised forms of conservation equations with variable *h*.

References

[1] Gingold R A and Monaghan J J Smoothed particle hydrodynamics: theory and application to non-spherical stars Mon. Not. R. Astron. Soc. 181 (1977) 375–89

[2] Benz W Smoothed particle hydrodynamics—a review The Numerical Modelling of Nonlinear Stellar Pulsations ed J R Buchler (Dordrecht: Kluwer) (1990) 269–88

[3] Monaghan J J Smoothed particle hydrodynamics Ann. Rev. Astron. Astrophys. 30 (1992) 543–74

[4] Larry D. Libersky, Albert G . Petschek, Theodor C. Carney, Jim R Hipp and Firooz A. Allahdadi, High Strain Lagrangian Hydrodynamics a Three-Dimensional SPH code for dynamic material response,. Journal of Computational Physics, 109 (1993) 67-75

ACCEPTED MANUSCRIPT

[5] Morris, J.P., An Overview of the Method of Smoothed Particle Hydrodynamics, November 1995, Universitat Kaiserlautern, Arbeitsgruppe Technomathematik.

[6] Bonet J and Lok T-S L Variational and momentum preservation aspects of smooth particle hydrodynamic formulations Comput. Methods Appl. Mech. Eng. 180 (1999) 97–115

[7] Monaghan J. J., Smoothed particle hydrodynamics, Rep. Prog. Phys. 68 (2005) 1703–1759

[8] Gelfand, I.M., Shilov, G.E., Generalized Functions, New York Academic Press, 1960.

[9] Belytschko T, Guo Y, Liu WK, Xiao SP. A unified stability analysis of meshless particle methods, Int. Journal for Numerical Methods in Engineering; 48: (2000) 1359-1400.

[10] Libersky L., Petschek. A. Smooth Particle Hydrodynamics with strength of materials, In Trease H., Fritts M., and Crowley W., editors, Advances in the Free-Lagrange Method, (1990) 248-257, Springer-Verlag.

[11] Hughes, T.J.R., Liu, W.K., Zimmermann, T.K., Lagrangian-Eulerian Finite Element Formulation for Incompressible Viscous Flows, Computer Methods in Applied Mechanics and Engineering, 29 (1981) 329-349.

[12] Richard P. N., Papaloizou J, C. B.;Variable Smoothing Lengths And Energy Conservation In Smoothed Particle Hydrodynamics, Monthly Notices of the Royal Astronomical Society, 270, (1994)

[13] Toro E.F. Riemann Solvers and Numerical Methods for Fluid Dynamics, Springer-Verlag, Berlin. (1997).

[14] Campbell J, Vignjevic R, Libersky L. A Contact Algorithm for Smoothed Particle Hydrodynamics, Computer Methods in Applied Mechanics and Engineering, 184 (2000) 49-65.

[15] Vignjevic R., Campbell J., Libersky L. A Treatment of Zero Energy Modes in the Smoothed Particle Hydrodynamics Method, Computer Methods in Applied Mechanics and Engineering, 184 (2000) 67-85.

[16] R. Vignjevic; Juan R. Reveles, James Campbell, SPH in a Total Lagrangian Formalism, Computer Methods in Engineering and Science, 14 (2006) 181-198.

[17] Belytschko T., Liu W.K. Moran B. Nonlinear Finite Elements for Continua and Structures. John Wiles sons Ltd. (2000)

ACCEPTED MANUSCRIPT

Figure Captions

Figure 1: Kernel support and neighbouring particles in the discrete kernel interpolation.

Figure 2: A 2D domain of a kernel function in the conventional SPH method

Figure 3: Deformation of the material referential volume Ω_0 and vector $2\mathbf{h}_0$ into a spatial volume Ω and vector $2\mathbf{h}$. (X_1, X_2, X_3) are the material coordinates, (x_1,x_2,x_3) are the spatial coordinates and ($x_1^{'}, x_2^{'}, x_3^{'}$) are the referential coordinates.

Figure 4: A 2D representation of domain of a kernel function in a moving coordinate system

Figure 5: Initial conditions of shock tube problem

Figure 6: Density profile for shock tube at time 0.2.

Figure 7: Pressure profile for shock tube at time 0.2.

Figure 8: Initial conditions for 2D block test problem

Figure 9: Comparison of *y*-velocity (cm/μs) at time 1.0 μs (a) Conventional SPH (b) New Framework..

Figure 10: Comparison of von Mises effective stress (Mbar) at time 1.0 μs. (a) Conventional SPH (b) New Framework..

Figure 11: Comparison of *y*-velocity (cm/μs) at time 2.5 μs. (a) Conventional SPH (b) New Framework..

Table Captions

Table 1: Material properties

Figure 1

ACCEPTED MANUSCRIPT

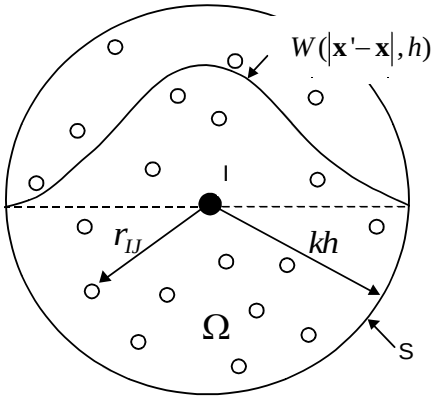


Figure 1: Kernel support and neighbouring particles in the discrete kernel interpolation.

ACCEPTED MANUSCRIPT

ACCEPTED MANUSCRIPT

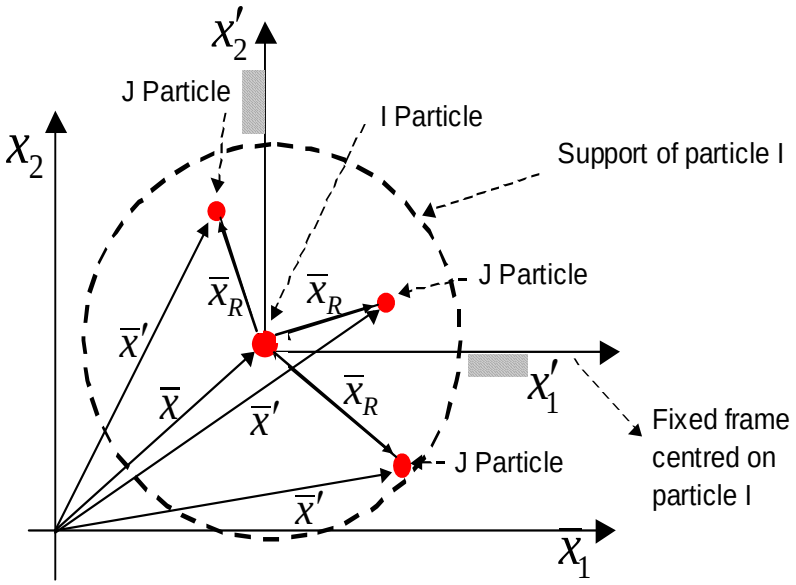


Figure 2: A 2D domain of a kernel function in the conventional SPH method

ACCEPTED MANUSCRIPT

Figure 3

ACCEPTED MANUSCRIPT

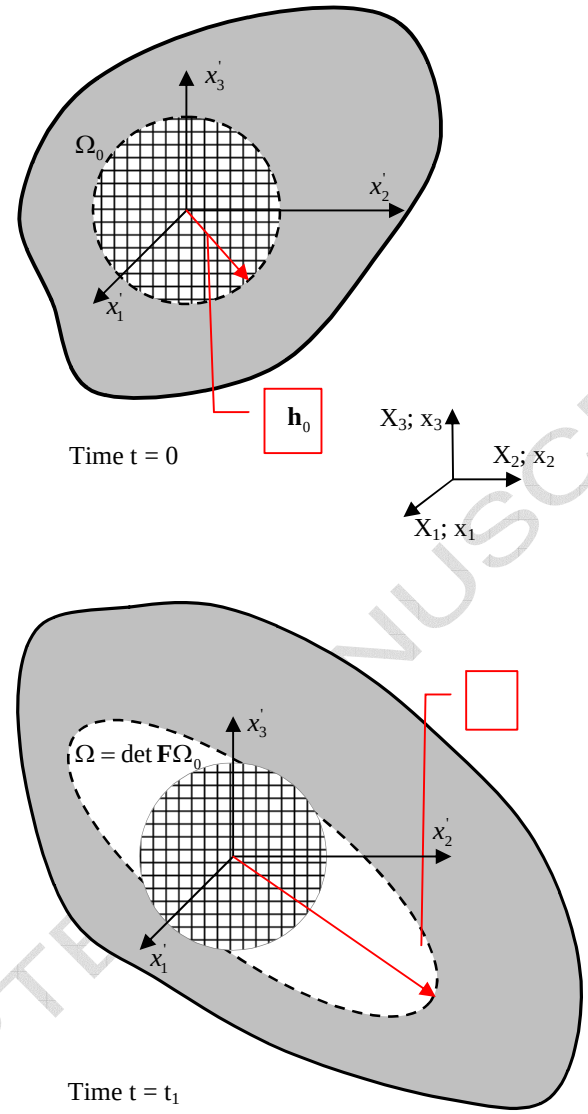


Figure 3: Deformation of the material referential volume Ω_0 and vector $2\mathbf{h}_0$ into a spatial volume Ω and vector $2\mathbf{h}$. (X_1, X_2, X_3) are the material coordinates, (x_1,x_2,x_3) are the spatial coordinates and (x_1', x_2', x_3') are the referential coordinates.

Figure 4

ACCEPTED MANUSCRIPT

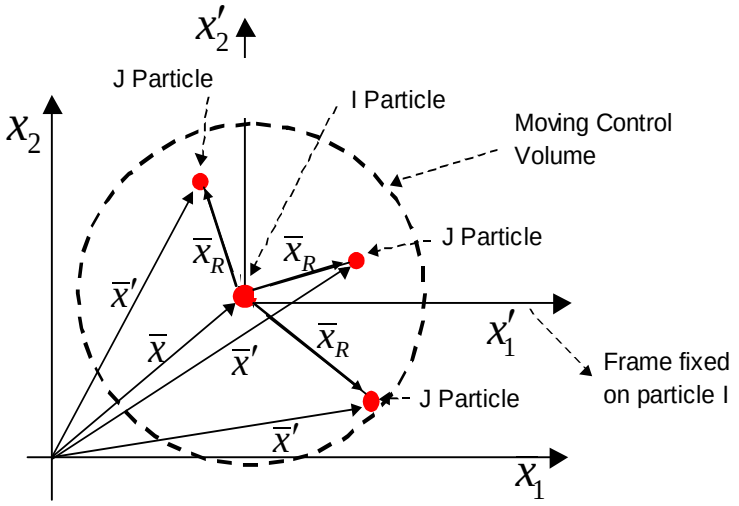


Figure 4: A 2D representation of domain of a kernel function in a moving coordinate system

ACCEPTED MANUSCRIPT

Figure 5

ACCEPTED MANUSCRIPT

Left	Right
$0 < x < 0.5$	$0.5 < x < 1.0$
$\rho_L = 1.0$	$\rho_R = 0.125$
$P_L = 1.0$	$P_R = 0.1$
$v_L = 0.0$	$v_R = 0.0$

Figure 5: Initial conditions of shock tube problem

ACCEPTED MANUSCRIPT

ACCEPTED MANUSCRIPT

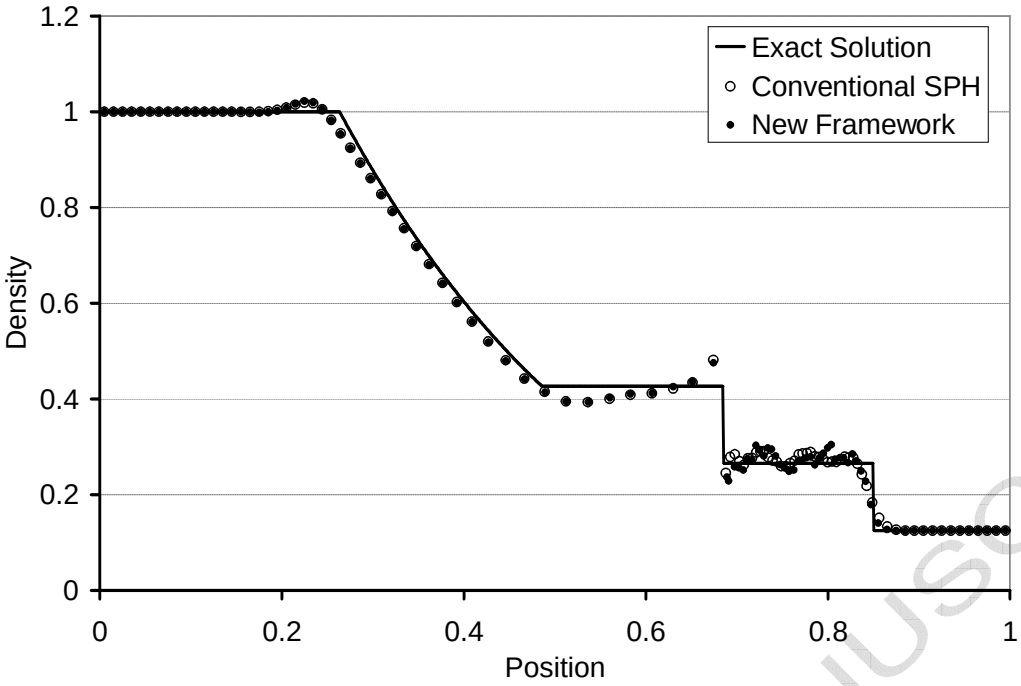


Figure 6: Density profile for shock tube at time 0.2.

ACCEPTED MANUSCRIPT

Figure 7

ACCEPTED MANUSCRIPT

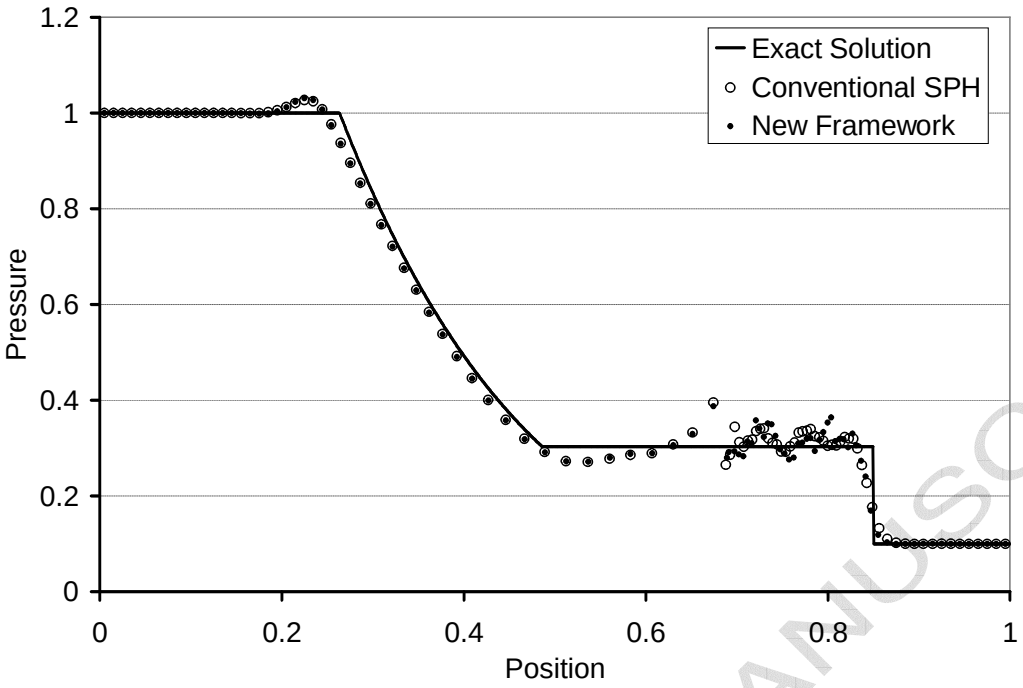


Figure 7: Pressure profile for shock tube at time 0.2.

ACCEPTED MANUSCRIPT

ACCEPTED MANUSCRIPT

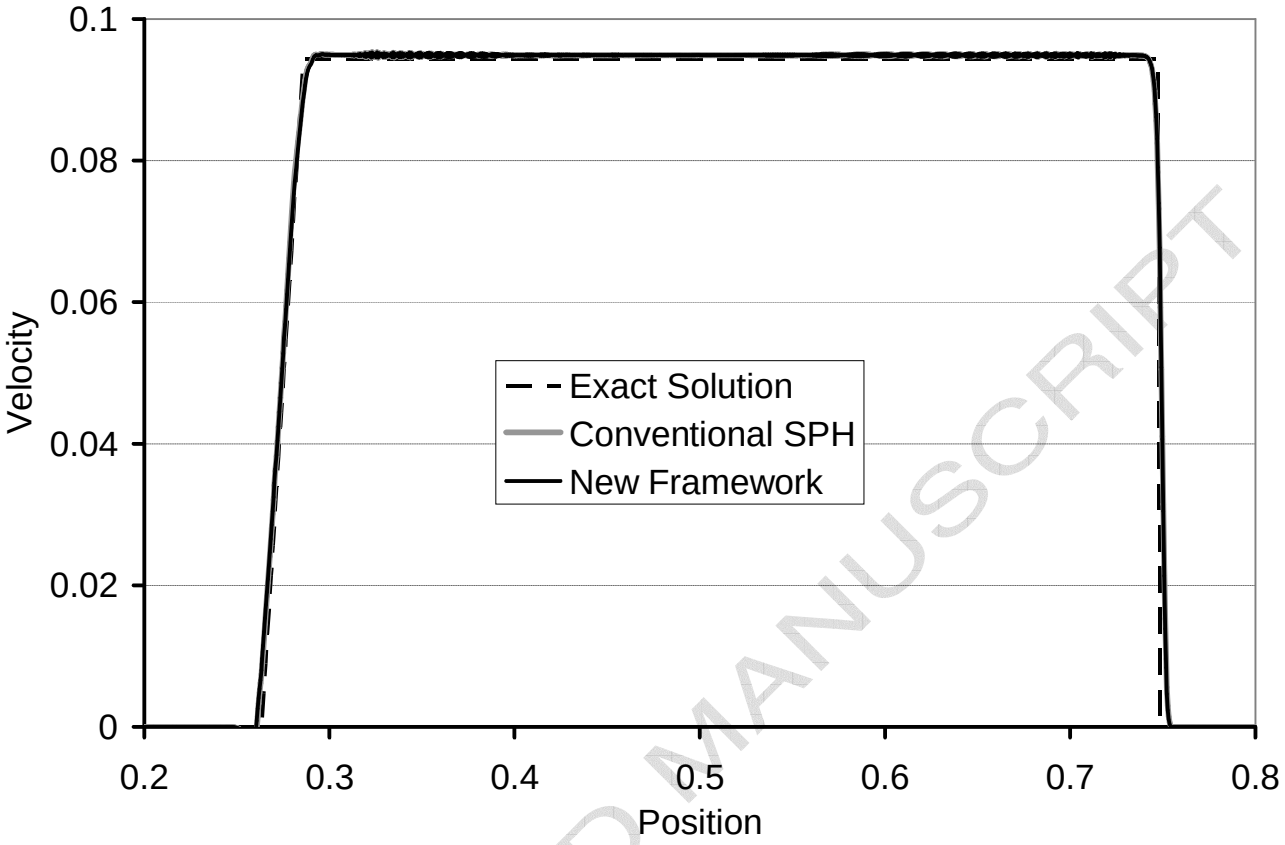


Figure 8: Velocity profile for shock tube at time 0.2.

ACCEPTED MANUSCRIPT

ACCEPTED MANUSCRIPT

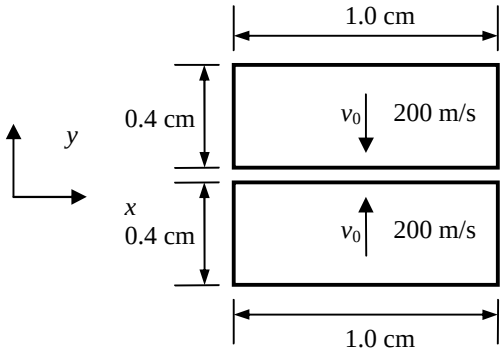


Figure 9: Initial conditions for 2D block test problem

ACCEPTED MANUSCRIPT

Figure 10 a

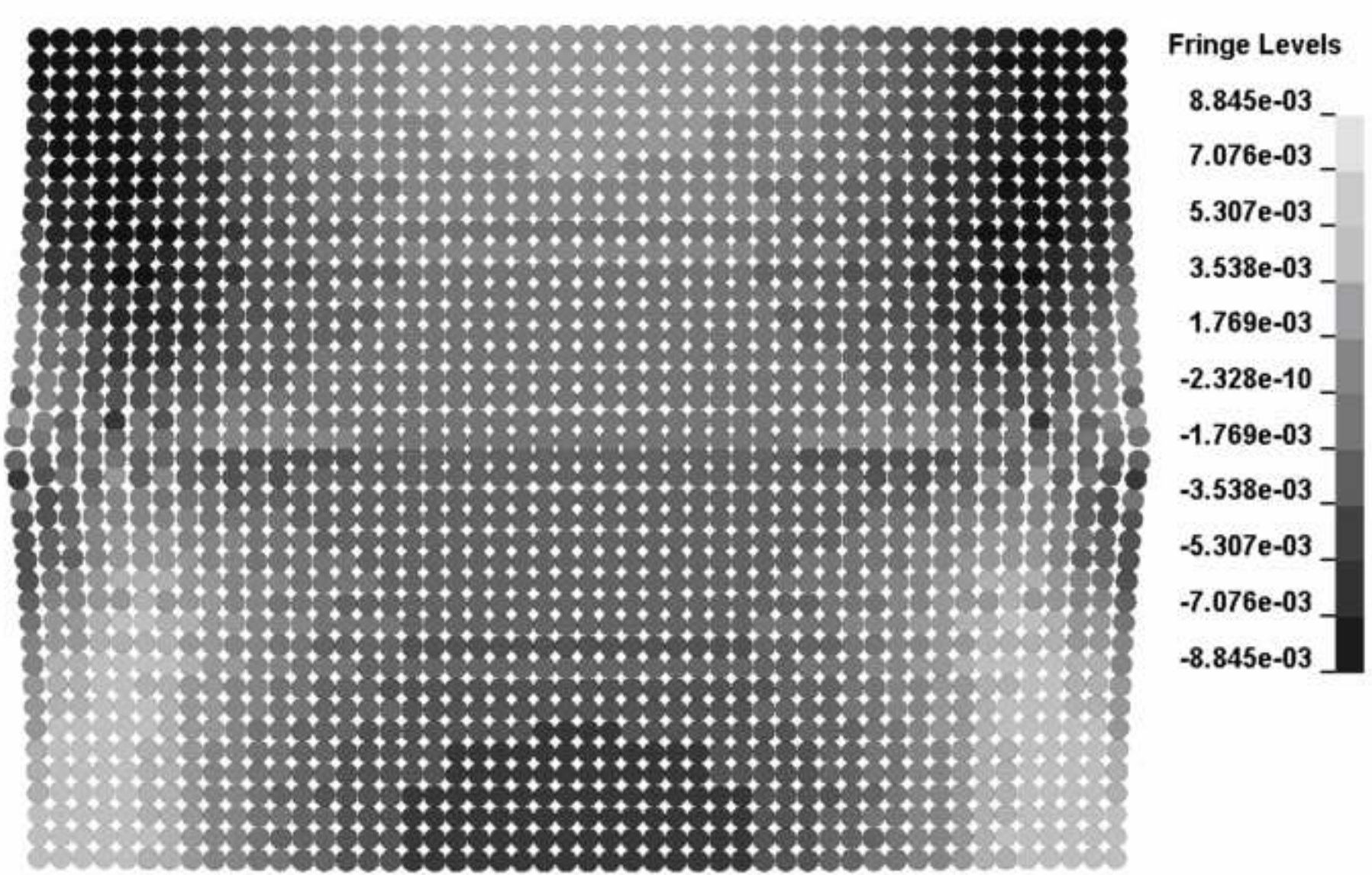

Fringe Levels
8.845e-03
7.076e-03
5.307e-03
3.538e-03
1.769e-03
-2.328e-10
-1.769e-03
-3.538e-03
-5.307e-03
-7.076e-03
-8.845e-03

Figure 10 b

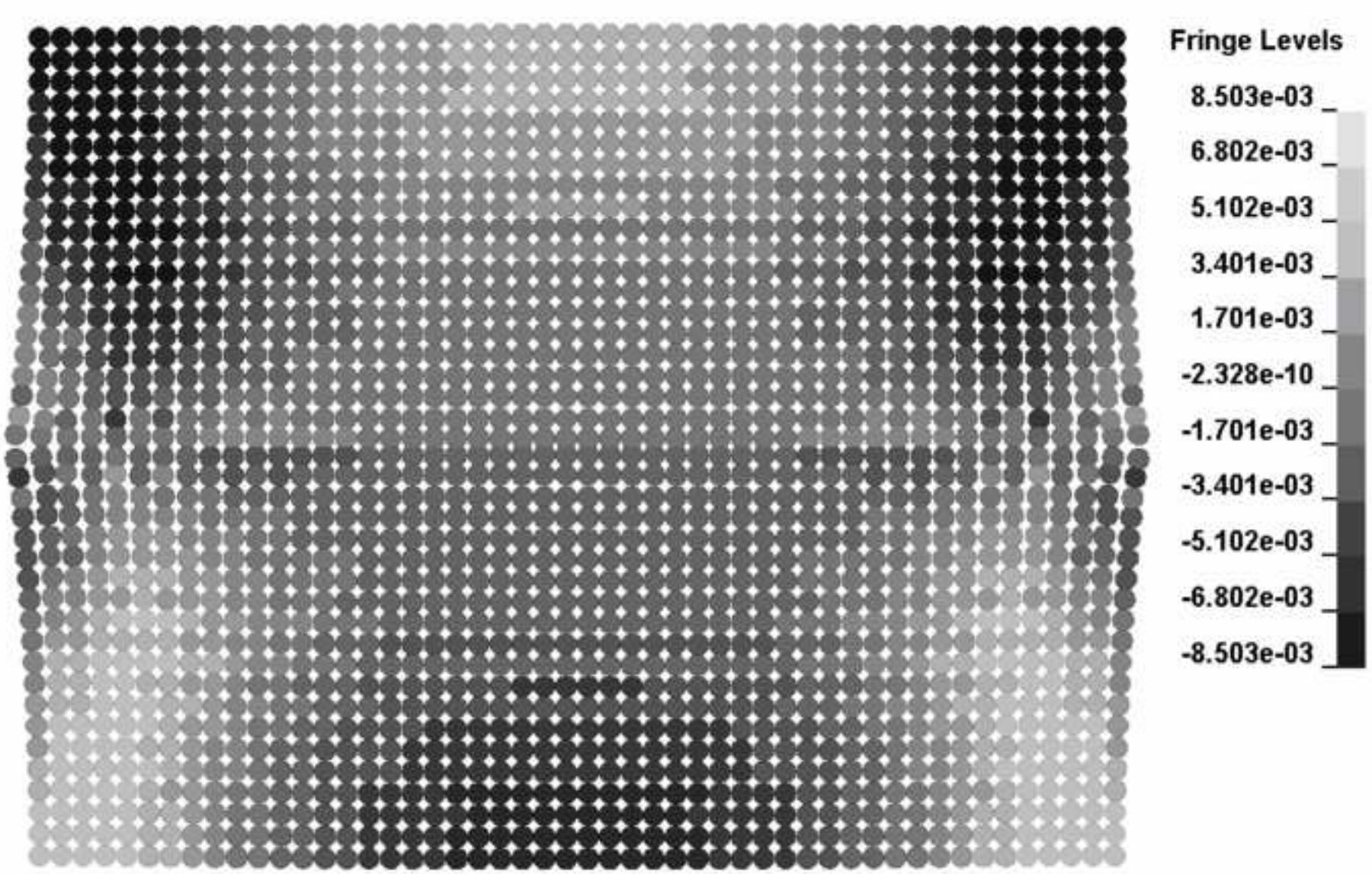

Fringe Levels
8.503e-03
6.802e-03
5.102e-03
3.401e-03
1.701e-03
-2.328e-10
-1.701e-03
-3.401e-03
-5.102e-03
-6.802e-03
-8.503e-03

Figure 11a

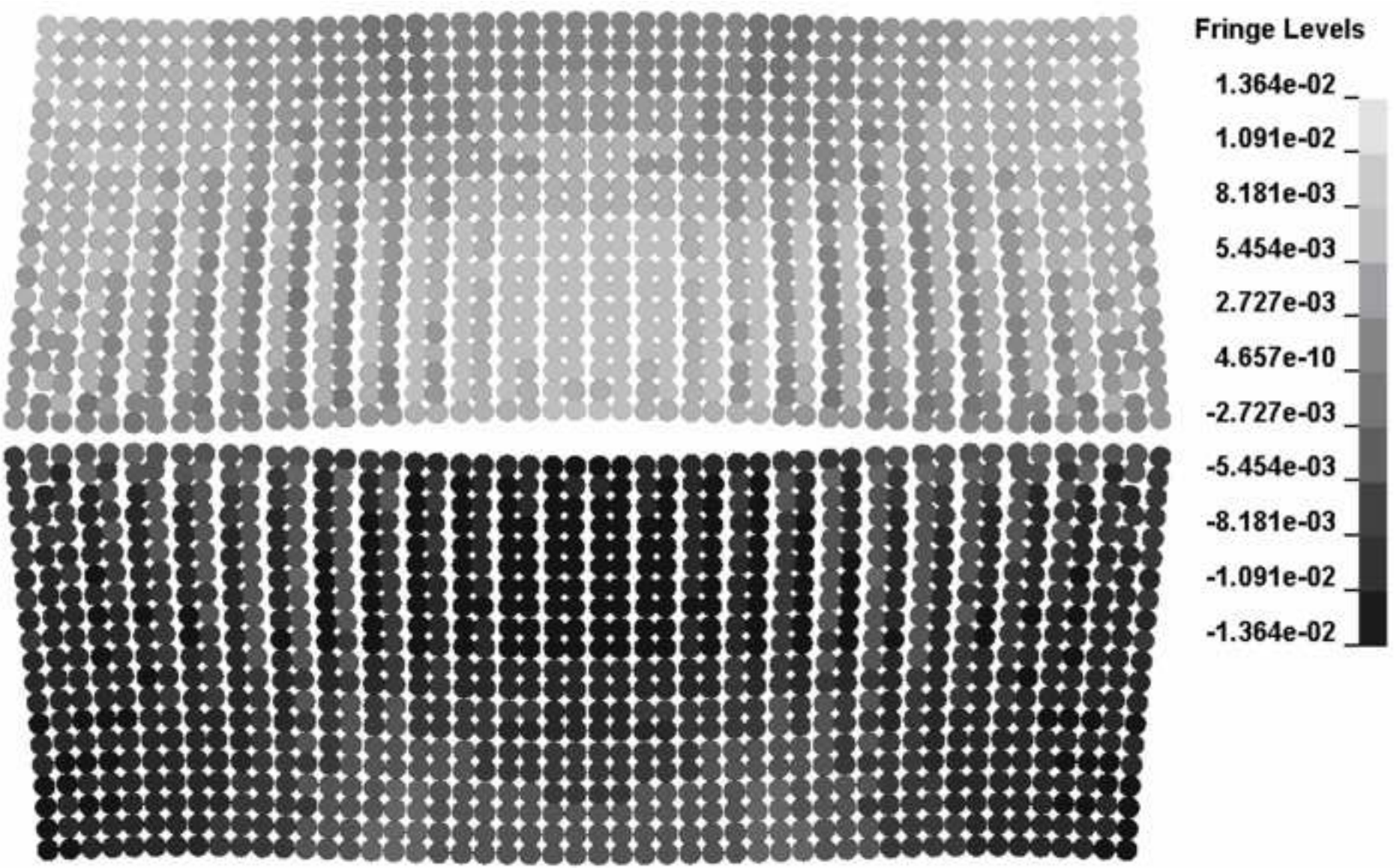
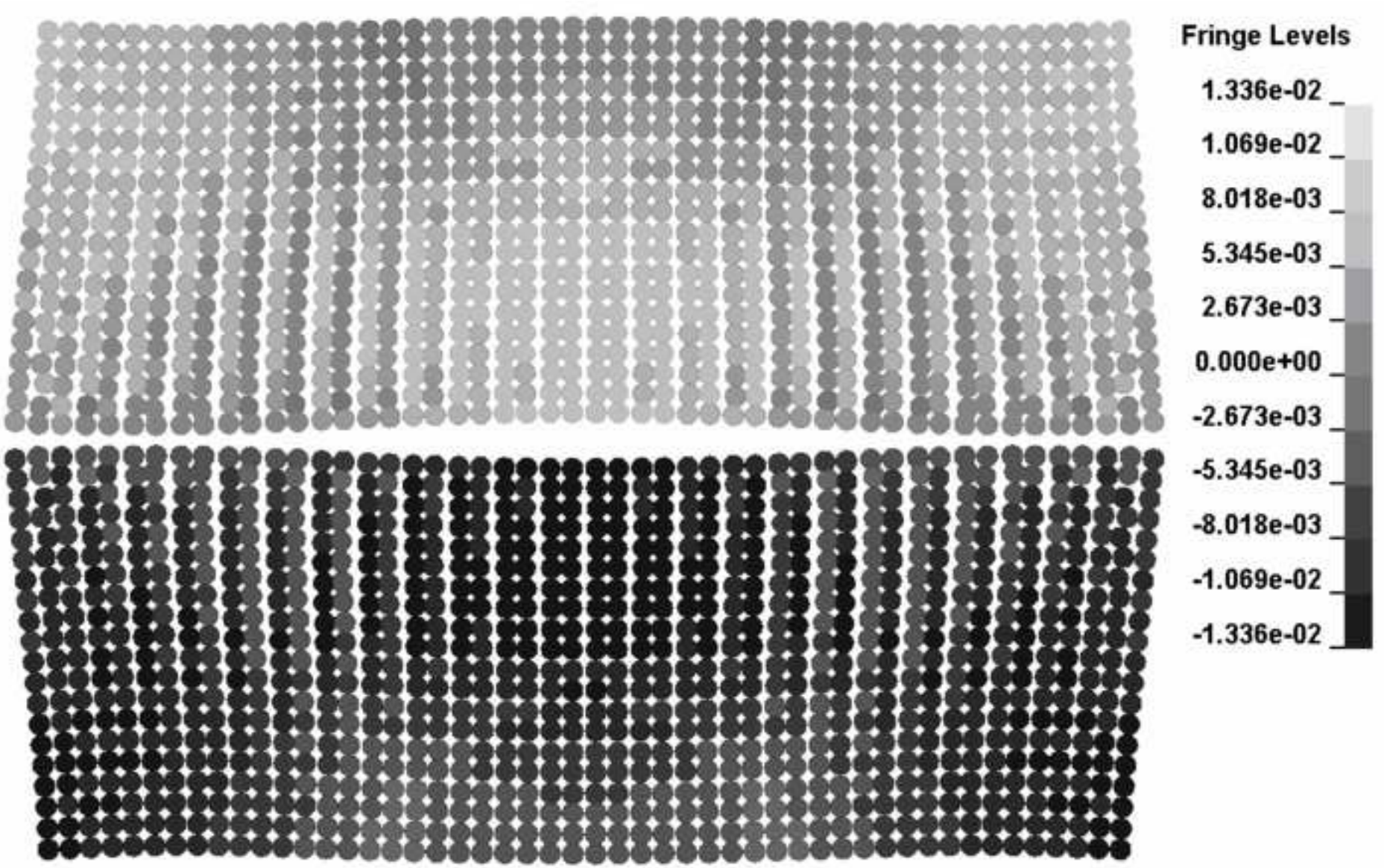

Fringe Levels
1.364e-02
1.091e-02
8.181e-03
5.454e-03
2.727e-03
4.657e-10
-2.727e-03
-5.454e-03
-8.181e-03
-1.091e-02
-1.364e-02

Figure 11b


Fringe Levels
1.336e-02
1.069e-02
8.018e-03
5.345e-03
2.673e-03
0.000e+00
-2.673e-03
-5.345e-03
-8.018e-03
-1.069e-02
-1.336e-02

ACCEPTED MANUSCRIPT

Table 1: Material properties

Density	7.8 g/cm^3
Elastic modulus	2.1 Mbar
Poisson's Ratio	0.3
Yield Stress	0.01 Mbar
Plastic tangent modulus	0.21 MBar

ACCEPTED MANUSCRIPT



https://dspace.org/

Derivation of SPH equations in a moving referential coordinate system

Vignjevic, Rade; Campbell, James C.; Jaric, J.; Powell, S.

2009-06-01T00:00:00Z
Elsevier Science B.V., Amsterdam.
http://dx.doi.org/10.1016/j.cma.2009.02.027
R. Vignjevic, J. Campbell, J. Jaric, S. Powell, Derivation of SPH equations in a moving referential coordinate system, Computer Methods in Applied Mechanics and Engineering, Volume 198, Issues 30-32, 1 June 2009, Pages 2403-2411

Downloaded from a DSpace repository. https://dspace.org/